

**Geophysical Investigations of Faults
in the Makgadikgadi Basin, Northern Botswana**

by

Landon Lockhart

B.S. Degree Candidate

Honors Senior Thesis

Presented to the Faculty of the Graduate School of Oklahoma State University
in Partial Fulfillment
of the Requirements
for the Honors Degree

Oklahoma State University

Spring 2015

Past publications have linked the southwest propagation on the East African Rift System (EARS) in northern Botswana to the surface faults and seismic activity in the Makgadikgadi Basin by speculation (Fig. 2). To our knowledge, no other publications have mapped the faults in the basement, thus no one has confirmed this proposition that rifting is occurring in the Makgadikgadi Basin. Because of the evidence of active seismicity and the clear northeast southwest of the surface faults (Figures 3b, 8, 12 a, b), our hypothesis is that the faults in the basement will coincide with the surface faults. This leads us to the

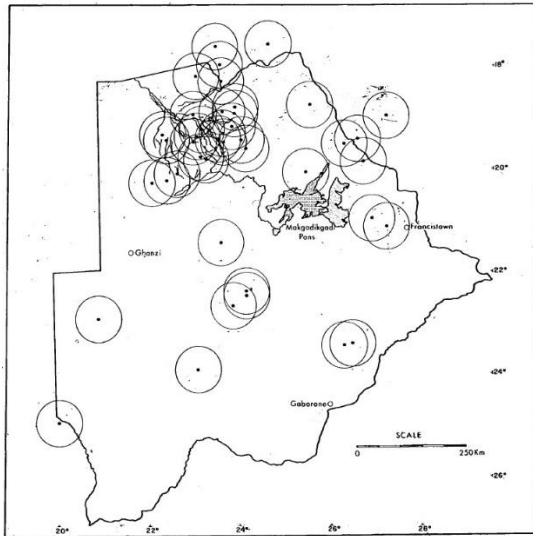


Figure 2: Map of northern Botswana. Circles with dots in center represent location of earthquake epicenters from 1965-1971 (Image after Ballieul, 1979).

purpose and motivation of this paper which is as follows: (1) to map the faults on the surface and in the basement and to determine if any correlation exists; (2) to determine the age of faulting; (3) to measure the fault displacement-length relationships; and (4) to map any structures that might suggest an extensional setting. By doing so, we hope to provide a better understanding of the region supported with evidence from our geophysical investigations.

Tectonics

Recently deposited sands with thicknesses up to 75 m cover the bedrock geology of the region, which is bounded on the south and east by Karoo-aged sandstone and basalt escarpments (Burrough et al., 2009). Undated granite and

migmatite outcrops exist in the area between the two pans where uplift has occurred (Ballieul, 1979). The rest of the area is underlain by Karoo sandstone and siliceous dolomite (Ballieul, 1979). The Okavango Dikes, which cut through the southern portions of the pans, and post-Karoo faulting have highly fractured the rocks around the pans (Ballieul, 1979). The predominant composition of the pans is clay and silt intermixed with sand (Ballieul, 1979). Researchers speculate that lake salinity would have increase over time, as no outlet has been discovered (Ballieul, 1979).

Tectonism involving crustal flexuring and subsidence resulted in the formation of the Makgadikgadi Basin (Podgorski et al., 2013). However, when tectonism began has not been established (Podgorski et al., 2013). To the west of the Ntwetwe Pan where the Okavango Swarms are located (Fig 1), the Thamalakane and Kunyere Faults have generated a graben bounded by northeast trending faults where the densest cluster of active seismicity is located (Fig. 2; Moore et al., 2012; Ballieul, 1979). There are speculations that faulting extending from the Kafue Flats into the Makgadikgadi Basin affected the shape of the present-day pans (Ballieul, 1979). To the northwest of the Makgadikgadi Basin the Bulozhi graben is bounded by the Mwamba and N'gonye Faults (Moore, 2012).

Data and Methods

To improve our understanding of the region and to determine if the surface faults extend into the basement, we used aeromagnetic data commissioned by the Geological Survey of Botswana in 1996. Data were acquired at an altitude of ~80 m along north-south lines with 250 m spacing and east-west tie lines with 1.25 km line spacing. To enhance the structures in the basement, we used Geosoft's "MAGMAP" filtering software and applied first-order vertical, horizontal, tilt, positive, and negative derivatives, in addition to analytical signal. Also, in order to penetrate the especially obtrusive Okavango Dike Swarms that cut through a large portion of our area (Fig. 3a), we used the upward continuations filter at 5 km, 7.5 km, 10 km, and 15 km, and then again applied the aforementioned filters. This allowed us to penetrate deeper into the subsurface and to remove the dikes (Fig. 3b). Basement faults were mapped by identifying low magnetic anomalies that cut/displaced structures. Despite the filters enhancing magnetic anomalies, they may have also increased noise in the area.

We obtained the SRTM data (Fig. 5) from Geosoft with 90 m spatial resolution to examine topographic features and to construct west-east topographic profiles. Using Geosoft's filtering software we applied the vertical, horizontal, and tilt derivatives. This enhanced surface features resulting from faults, sand dunes, and the PLM shoreline. Surface faults were mapped by identifying linear structures that cut/displaced topographic features.

Results

(i) Fault Mapping from Aeromagnetic Data

Part of our first objective was to map the faults in the basement. Our data reveals deep-seated negative magnetic anomalies with low wavelength values reflecting a northeast trend. The largest clusters of faults occur in the northeast portion of the basin overlain by the Ntwetwe Pan. Many smaller faults intersect the Okavango Dike Swarm (Fig. 6), which underlie most of the southern portions of the pans. An especially long fault of >200 km extends between the two pans.

Part of our second objective was to investigate cross-cutting relationships so we could establish the relative age of faulting. As seen in Figure 6, various faults are clearly displacing parts of the Okavango Dike Swarm. Faulting has displaced various dikes and left others unaltered, which could be the result of dip-slip faulting cutting the vertical dikes. From our data, we can ascertain the faults postdate the dikes.

Our third objective was to determine displacement-length relationships. From one fault (Fig. 7) in the northeastern portion of the study area, we were able to determine fault displacement in the basement of ~150 m. However, due to time constraints with this

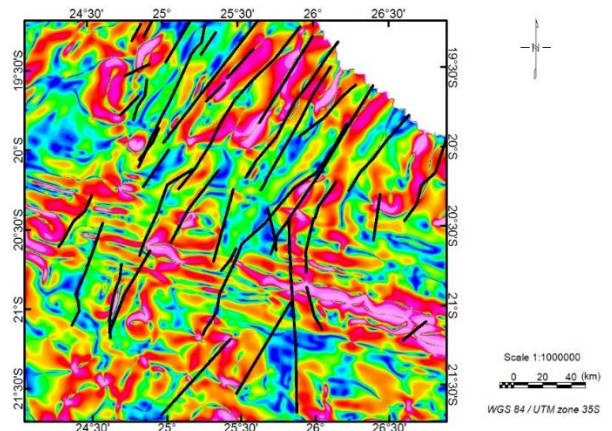


Figure 3: Aeromagnetic image of the Makgadikgadi Basin created from the upwards continuation at 7.5 km and horizontal tilt derivative filters.

project, we were unable to investigate any further the basement displacement of nearby faults. Consequently we focused more time on the geometry of the surface faults, as our SRTM data results reveal.

(ii) Fault Mapping from SRTM Data

By applying different filters to our SRTM data (Fig. 8), we mapped the surface faults and created topographic profiles of some of the longer faults (Fig. 9 a, b). Our results indicate the largest cluster of faulting is occurring in the northern part of the basin with a clear northeast trend. Previous papers that have mapped the surface faults of the Makgadikgadi Basin coincide with our results, giving us confidence in our work (Podgorski et al., 2013; Ballieul, 1979; Moore et al. 2012).

Once again, as in the aeromagnetic data, we applied the basic principles of cross-cutting relationships to establish the relative age of faulting for our second objective. It is clear from our data that the PLM shoreline cuts the Alab dunes (Fig 4). Moreover, the faults cut both the shoreline and dunes. Figure 4 shows fault D-D' cutting the dunes. Our data further indicates the southeastern hanging wall on fault D-D' has dropped.

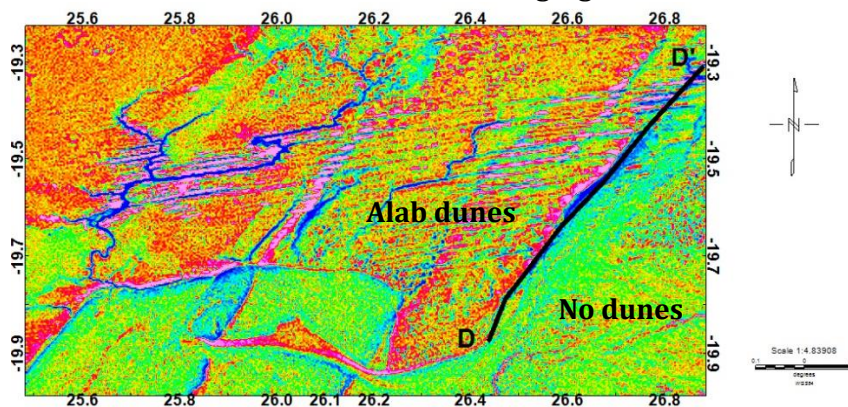


Figure 4: SRTM image of normal fault D-D' displacing the Alab dunes with vertical derivative filter.

normal faulting, resulting in erosional sediments covering the lower laying displaced dunes southeast of the fault.

Our third objective was to measure the displacement-length relationships. We measured the lengths of two of the longest faults, A-A', and B-B', and nearby faults C-C' and D-D' to get an idea of the geometry. Fault A extends for ~113

km and cuts the northeast border of the Ntwetwe Pan (Fig. 9 a). Maximum displacement is ~25m, with minimum displacement of ~5 m. Fault B is ~87 km has a maximum displacement of ~12 m and minimum displacement of ~4 m (Fig. 9 b). However, this fault may extend further southwest along the northeast border of the Sua Pan, giving it a total length of ~186 km. The length of fault C is estimated to be ~41 km with maximum displacement of ~45 m and minimum ~14 m (Fig 9 b). Finally, fault D extends for ~58 km with a maximum displacement of ~40 m and a minimum displacement of ~8 m (Fig. 9 a). Figure 14 summarizes these results.

Our fourth and final objective was to map any structures in the area that might suggest an extensional setting. In the northern portion of the Ntwetwe Pan we discovered a small graben (Fig 10 a). Our topographic profiles (Fig 10 b) indicate a portion of the Ntwetwe Pan that has undergone subsidence, which formed this graben. We also discovered in the

northeastern portion of the Makgadikgadi Basin a small horst with sharp escarpments (Fig. 11 a). Normal faulting caused by uplift displaced the older PLM shoreline and resulted in this horst.

Discussion and Conclusions

Our first objective was to map the fault in the basement and on the surface and determine if any correlation exists. From our results we were able to determine a clear northeast trend. Additionally, we found that many more faults occur in the basement than on the surface. What is most interesting is the correlation between the surface and basement faults (Fig 12 a, b). We discovered that each of the surface faults extend into the basement, thus providing evidence that the surface faults are undergoing reactivation from the basement faults. However, the numerous lengthy basement faults that have not been reactivated on the surface present a particularly dangerous threat. The unactivated basement faults could result in serious earthquakes in the future.

Our second objective was to determine the age of faulting. By establishing cross-cutting relationships and drawing upon different topographic features that have been dated in previous publications, we were able to determine the faults cut the Okavango Dikes Swarm (~180 m.y.a), the Alab dunes (~200,000 B.P.) and the PLM shoreline (age unknown) (Ballieul, 1979; LePera, et al., 2014). Thus we are able to conclude the faults postdate the dikes, dunes, and shoreline. Because the Alab dunes are the youngest dated topographic feature that has been displaced by faulting, we can establish with confidence the faults are younger than 200,000 B.P.

Our third objective was to measure the fault displacement-length relationships. We discovered that the most displacement occurred in the northeastern portion of the faults and gradually decrease as the faults extend southwest, creating a gradient. This indicates the faults are propagating southwest. We also discovered that these very long surface faults show very little displacement. The displacement-length relationships of the Makgadikgadi Basin faults are inconsistent with past models (Kim et al., 2005).

Extensive studies have attempted to explain fault geometry based on the relationship between maximum displacements against lengths. A linear relationship exists, as seen in Figure 13, with our displacement-length values plotted against a previous model (Kim et al., 2004). Figure 14 shows faults A-A', B-B', C-C', and D-D' with their maximum length (km), displacement (m), and expected range of maximum displacement (m) (Kim et al., 2004). It is clear from our results that these faults lay considerably far from the expected maximum displacement ranges, aside from fault C-C'. We suggest such little displacement is a result of either erosion of the escarpments or from tectonic memory. If it were the latter, this would support the idea from Ballieul (1979) that renewed tectonic activity is occurring in zones of crustal weakness. This abnormal relationship offers a framework for future studies.

Our fourth and final objective was to map any structures that might suggest an extensional setting. From our SRTM topographic profiles we discovered a small graben (Fig. 9 a, b) and horst (Fig 10 a, b). The size of these structures indicates little expansion

over a wide zone of extension (~220 km), thus providing evidence that extension is occurring in the Makgadikgadi Basin. This supports the idea that rifting is occurring in the Makgadikgadi Basin. However, more studies utilizing other geophysical methods like gravity need to be investigated before concluding if this is indeed an area of rifting.

To our knowledge, this is the first geophysical investigation of the Makgadikgadi Basin. Our data indicates the basin is an extensional setting with highly abnormal fault geometry and still more questions unanswered. Further investigations are needed to link the faulting with the East African Rift System, and we hope our results prompt future studies.

Appendix

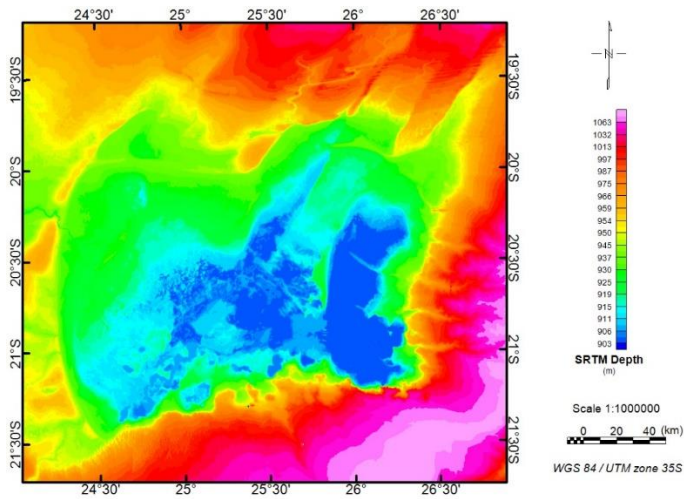


Figure 5: SRTM image of Makgadikgadi Basin.

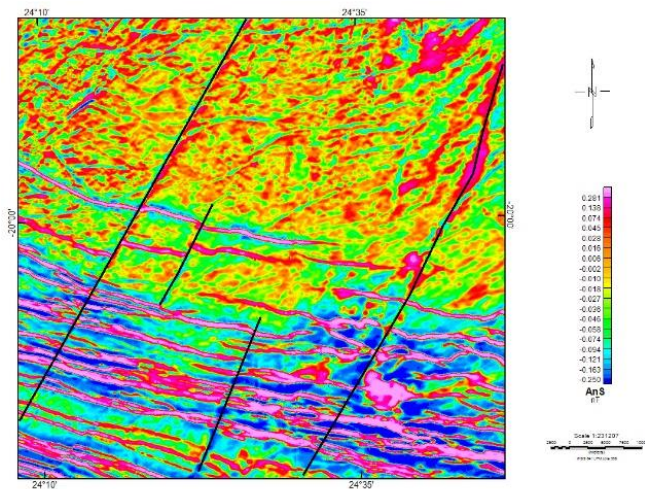


Figure 6: Aeromagnetic image of faults displacing Okavango Dike Swarm with analytical signal filter.

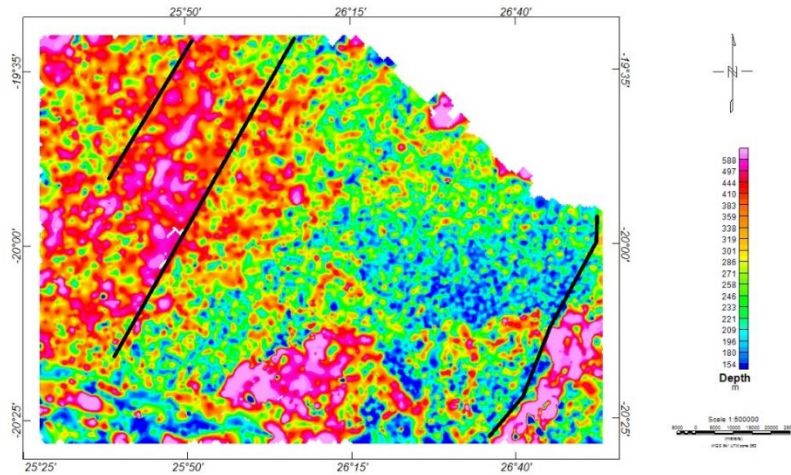


Figure 7: Aeromagnetic image of basement displacement from located Euler deconvolution.

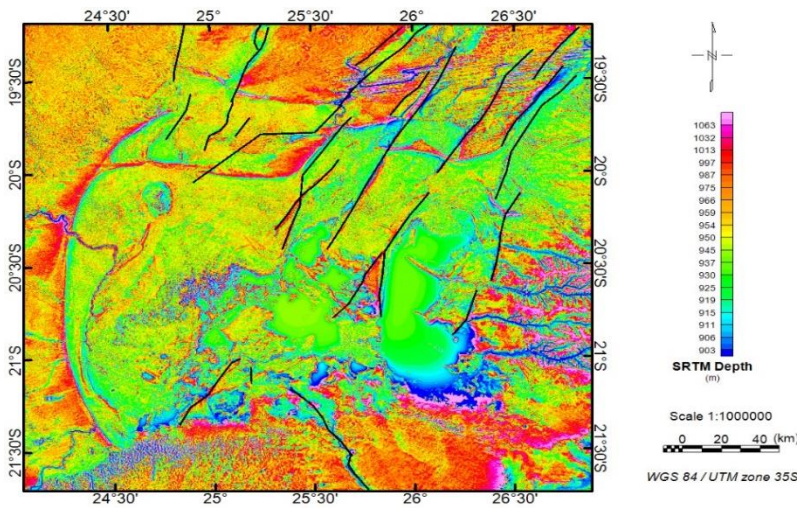
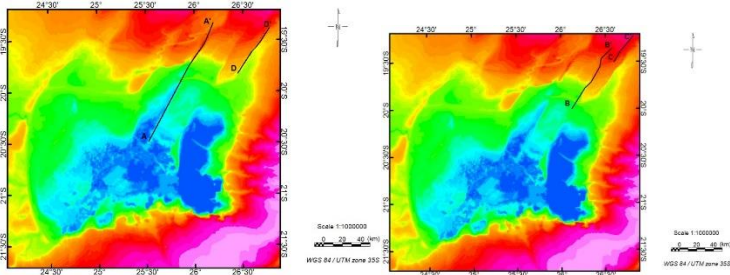
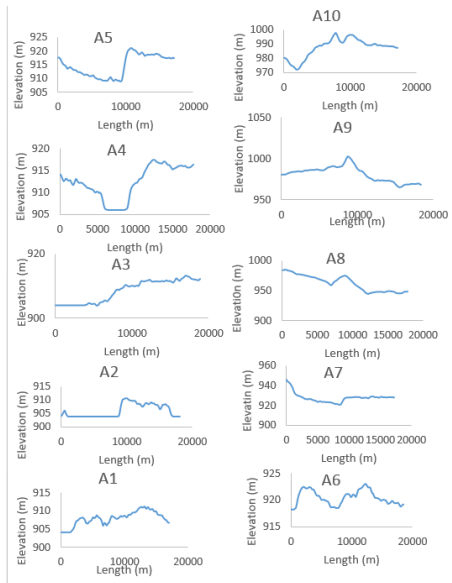


Figure 8: SRTM image of Makgadikgadi Basin with faults and vertical derivative filter.

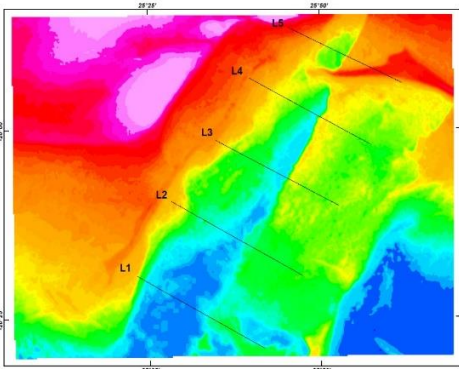


a)

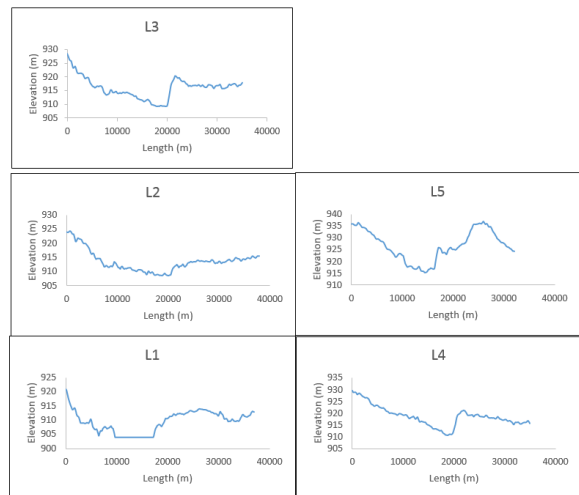


b)

Figure 9: (a) SRTM image of Makgadikgadi Basin with faults A-A' and D-D'. (b) Topographic profiles with elevation (m) against length (m) of fault A-A'.



a)



b)

Figure 10: (a) SRTM image of a small graben in the northernmost portion of the Ntwetwe Pan with profiles L1-L5. (b) Topographic profiles L1-L5 with elevation (m) against length (m) of graben.

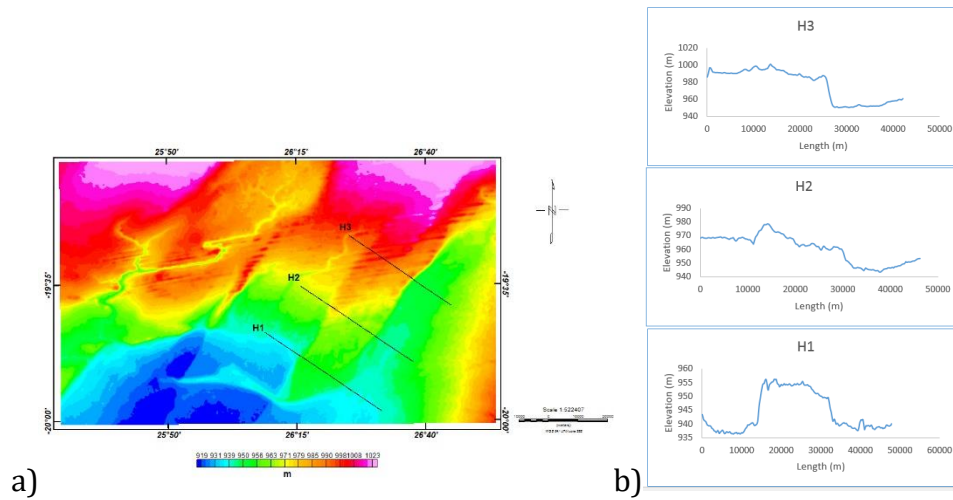


Figure 11: (A) SRTM image of a small horst in the Makgadikgadi Basin with profiles H1-H3. (B) Topographic profiles H1-H3 with length (m) vs elevation (m) of horst.

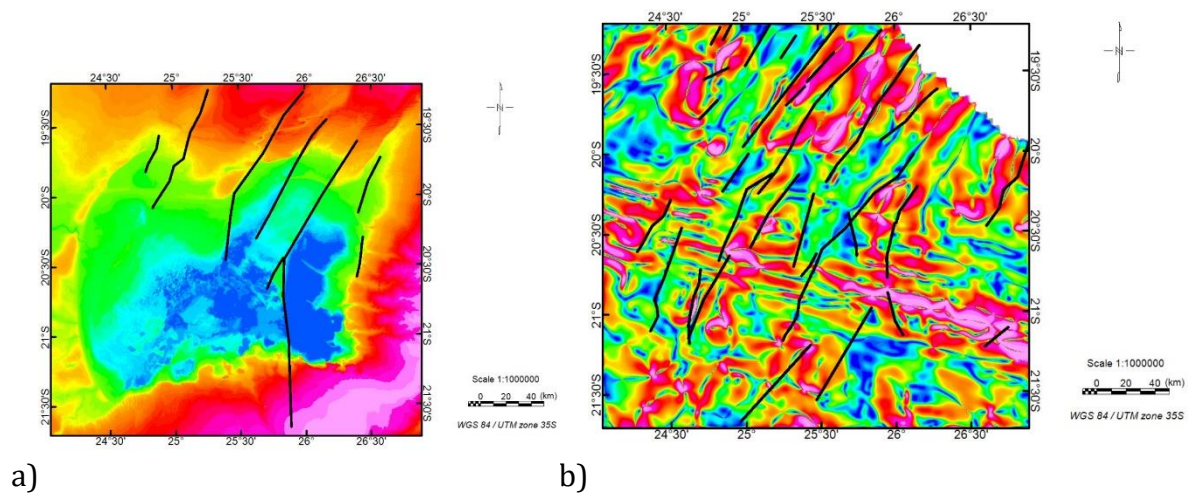


Figure 12: (a) Composite image of faults from SRTM and Aeromagnetic data. (b). Image of faults from magnetic data that do not appear in SRTM.

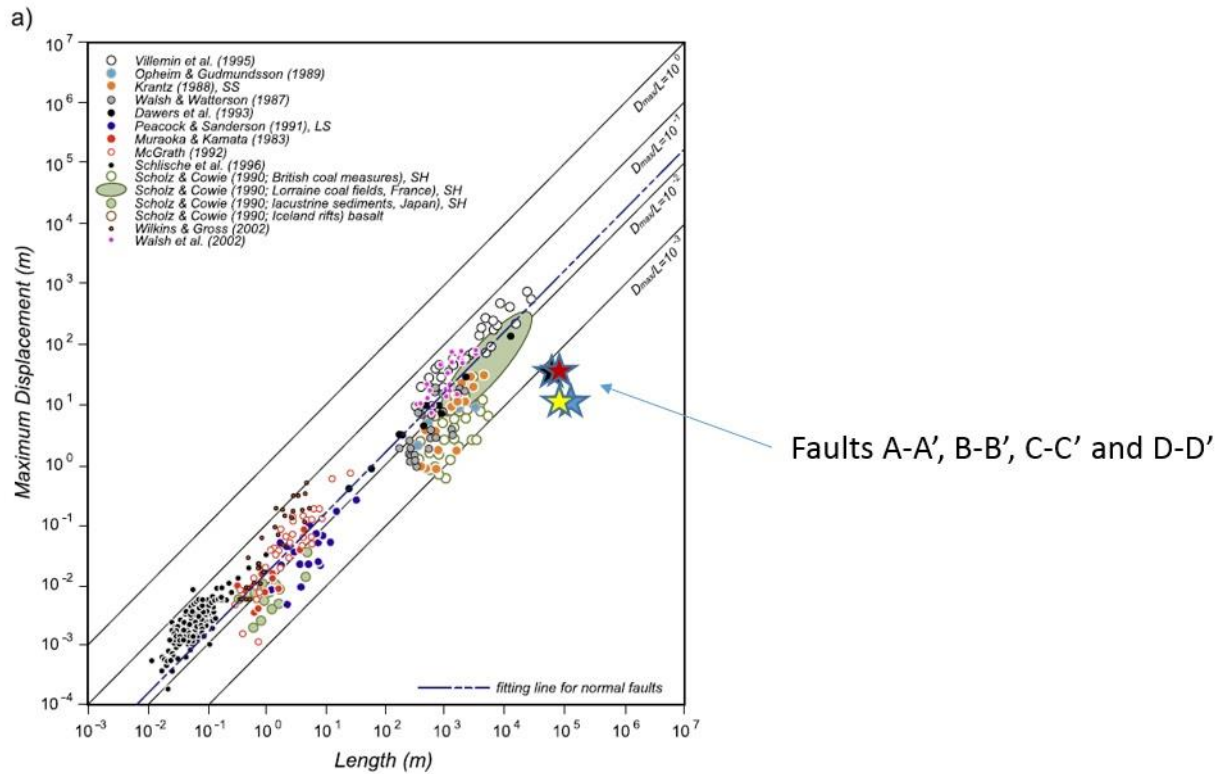


Figure 13: Plot of maximum displacement (m) against length (m) for normal, thrust, and strike-slip faults. Stars indicate where faults A-A', B-B', C-C', and D-D' plot against accepted model (Image after Kim et al., 2005).

Fault	Length (km)	Maximum Displacement (m)	Expected Range of Maximum Displacement (m)
A	~113	~25	113-113,000
B	~87	~12	87-87,000
C	~41	~45	41-41,000
D	~58	~40	58-58,000

Figure 14: Summary of faults A-A', B-B', C-C', and D-D'. Graph includes measured fault length (km), maximum displacement (m), and range of values from Kim et al. (2005)'s model.

Acknowledgements

This project was funded by the National Science Foundation – Continental Dynamics grant # EAR 1255233 with REU supplement. The Geological Survey of Botswana allowed free access to the airborne magnetics data. Thanks to the Boone Pickens School of Geology and OSU for providing me with the scholarships and funding that enabled me to focus my time and energy on my academics and this project. Most importantly, thanks to all those who helped me with this project. Many thanks to my thesis advisor Professor Estella Atekwana and to Professor Mohamed Abdelsalam for offering me guidance, advice, and your time. Thank you to Kitso and Andrew for spending countless times teaching me Geosoft; and to Tadessa for helping me with Landsat and Radarsat

References

- Ballieul, T.A. 1979. Makgadikgadi Pans complex of central Botswana. *Geological Society of America Bulletin*, 90, 289-312
- Campbell, G., et al. "Airborne geophysical mapping of aquifer water quality and structural controls in the Lower Okavango Delta, Botswana." *South African Journal of Geology* 109.4 (2006): 475-494.
- LePera, Alan, Estella Atekwana, and Mohamed Abdelsalam. "The Okavango Dike Swarm (ODS) of Northern Botswana: Was it associated with a failed Rift System?." *EGU General Assembly Conference Abstracts*. Vol. 16. 2014.
- Kim, Young-Seog, and David J. Sanderson. "The relationship between displacement and length of faults: a review." *Earth-Science Reviews* 68.3 (2005): 317-334.
- Moore, A. E., et al. "The evolution and ages of Makgadikgadi palaeo-lakes: Consilient evidence from Kalahari drainage evolution South-Central Africa." *South African Journal of Geology* 115.3 (2012): 385-413.
- Podgorski, Joel E., et al. "Paleo-megalake and paleo-megafan in southern Africa." *Geology* 41.11 (2013): 1155-1158.